Iran J Nucl Med. 2024;32(1):66-73 [Serial No. 62]

Homepage: https://irjnm.tums.ac.ir/

ORIGINAL RESEARCH ARTICLE

Radiomics analysis on blood-pool phase of bone scintigraphy for the diagnosis of Juvenile Idiopathic Arthritis

Marzieh Ebrahimi[1,2], Zeinab Paymani[2,3], Mostafa Nazari[2], Hossein Kian Ara[4], Nafiseh Alemohammad[4], Fatemeh Tahghighi Sharabian[5], Molood Gooniband Shooshtari[1]

[1]*Department of Medical Physics, School of Medicine, Iran University of Medical Sciences, Tehran, Iran*

[2]*Department of Nuclear Medicine, Children's Medical Center, Tehran University of Medical Sciences, Tehran, Iran*

[3]*Research Center for Nuclear Medicine, Tehran University of Medical Sciences, Tehran, Iran*

[4]*Department of Mathematics and Computer Science, Shahed University, Tehran, Iran*

[5]*Department of Pediatric Rheumatology, Children's Medical Center, Tehran University of Medical Sciences, Tehran, Iran*

ARTICLE INFO

Article History:
Received: 05 November 2023
Revised: 12 December 2023
Accepted: 13 December 2023
Published Online: 21 December 2023

Keyword:
Juvenile Idiopathic Arthritis
Nuclear medicine
Machine learning
Bone scintigraphy

*Corresponding Author:
Dr. Zeinab Paymani
Address: Department of Nuclear Medicine, Children's Medical Center, No. 62, Dr Gharib St, Tehran, Iran
Email: paymaniz@yahoo.com

ABSTRACT

Introduction: Diagnosing Juvenile Idiopathic Arthritis (JIA) presents challenges due to symptom variations, clinical-radiologic delays, and the absence of definitive diagnostic tools. This study aimed to evaluate the diagnostic capability of radiomic features derived from blood pool phase images obtained through bone scintigraphy in JIA.

Methods: A cohort of 190 patients was included, utilizing the area between knee growth plates as the region of interest (ROI) for extracting image features. After preprocessing, quantitative features were extracted from original and filtered images. A recursive feature elimination (RFE) algorithm identified significant features, subsequently employed in training a random forest classifier.

Results: In the validation phase, our radiomic model, comprising 14 features (4 original and 10 filtered image features), achieved an area under the receiver operating characteristic curve (AUC) of 0.89 (95% CI: 0.88–0.92). This robust performance confirmed the efficacy of radiomics in identifying active knee arthritis using technetium–99m-methyl diphosphonate blood pool images in JIA patients.

Conclusion: This study highlights the diagnostic accuracy of radiomics in discerning arthritic joints, suggesting its potential as an alternative to conventional quantification techniques. The robustness of radiomics in diagnosing arthritic joints signifies a promising avenue for future research in JIA diagnosis and treatment.

Use your device to scan and read the article online

How to cite this article: Ebrahimi M, Paymani Z, Nazari M, Kian Ara H, Alemohammad N, Tahghighi Sharabian F, Gooniband Shooshtari M. Radiomics analysis on blood-pool phase of bone scintigraphy for the diagnosis of Juvenile Idiopathic Arthritis. Iran J Nucl Med. 2024;32(1):66-73.

https://doi.org/10.22034/IRJNM.2023.129449.1584

INTRODUCTION

Juvenile Idiopathic Arthritis (JIA) manifests as joint inflammation in children under 16 years old, characterized by chronic autoimmune reactions targeting the joints. The resultant symptoms—swelling, stiffness, inflammation, and discomfort—underscore the necessity for early detection and treatment to prevent joint damage and related complications [1]. A gold standard for diagnosing JIA is conventional radiography. However, its limitations in sensitivity have prompted extensive efforts to develop more refined radiographic scoring systems. Currently, clinical assessment by rheumatologists is pivotal, relying on a comprehensive evaluation of symptoms, physical findings, laboratory results, and imaging studies. While Magnetic Resonance Imaging (MRI) is considered highly sensitive in identifying synovial pathologies, particularly in early stages, its capacity is limited in systemic rheumatologic disorders due to confined imaging field, often focusing on specific joints rather than offering a holistic assessment. The absence of a single gold standard test underscores the challenges in diagnosing JIA. This necessitates ongoing research into other refining diagnostic methodologies for future including nuclear medicine to enhance diagnostic precision and expedite early intervention [2-10]. Bone scintigraphy with technetium–99m-methyl diphosphonate ([^{99m}Tc] Tc-MDP) stands as a favored alternative due to its capacity for holistic joint evaluation, distinguishing arthritis and soft tissue inflammation, while ruling out other skeletal pathologies like trauma and metastasis [11, 12].

This modality comprises two phases: an initial capillary blood pool phase image and delayed bone metabolism views, offering valuable insights into diagnosing inflammatory pathologies [13, 14].

Radiomics, an advanced field, employs computational techniques to quantitatively analyze medical imaging, unveiling patterns beyond human perception while ensuring more objective and consistent outcomes [15-17].

Joint blood pool spot images in two-phase radionuclide bone scanning present advantages over other techniques—such as ultrasonography and MRI—offering comprehensive whole-body joint assessments in a single procedure, coupled with high sensitivity, availability, and cost-effectiveness [18]. Notably, the blood pool phase is particularly instrumental in detecting early-stage active joint inflammation [14, 18, 19]. To our knowledge, this study pioneers the utilization of radiomics on blood pool images for diagnosing JIA, aiming to explore the diagnostic potential of radiomic features in the blood pool phase of bone scintigraphy for JIA diagnosis.

METHODS

Study flowchart

Figure 1 illustrates the various stages undertaken in this study, encompassing image acquisition, image segmentation, feature computation, machine learning modeling, and model evaluation.

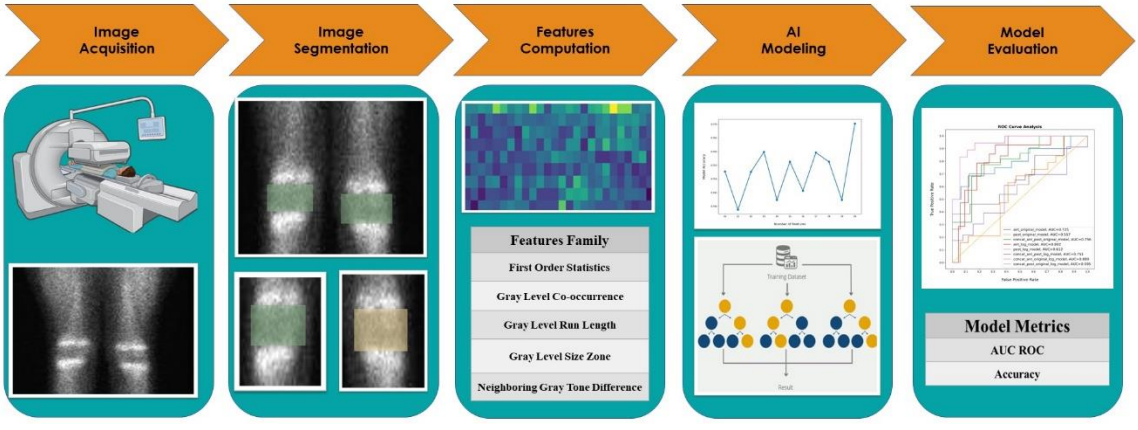

Figure 1. Radiomics study flowchart

Patient population

At the dedicated pediatric rheumatology clinic in the Children's Medical Center Hospital, a diverse range of JIA cases were referred for bone scintigraphy, aimed at detecting both active and silent arthritis manifestations. This retrospective cohort study, conducted at the Nuclear Medicine Department between 2021 and 2022, involved 190 patients (100 males and 90 females) with a mean age of 8 ± 3.5 years. The inclusion requires was clinically approved juvenile idiopathic arthritis (JIA) in at least one knee. Exclusion criteria were age

greater than 16 years and poor-quality images. Figure 2 shows the research flow diagram and patient inclusion with STARD criteria [20].

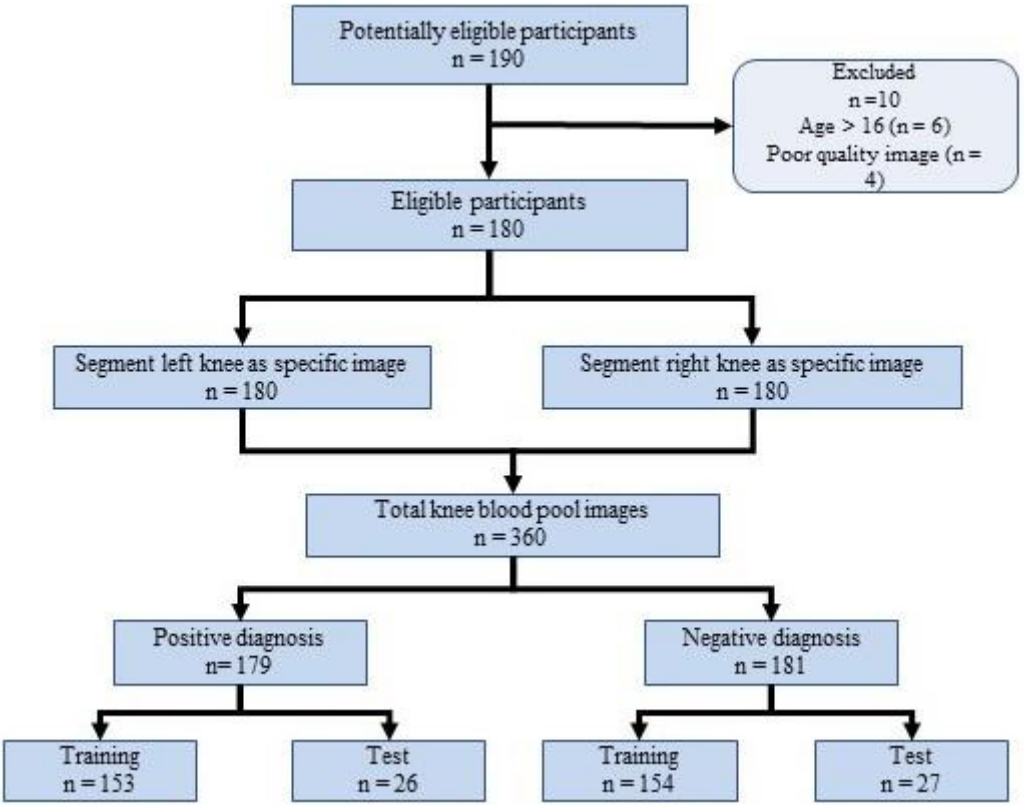

Figure 2. Study flow and patients' inclusion according to STARD criteria

Image acquisition and diagnostic validation

Imaging was performed with a dual-head gamma camera (Symbia Intevo Bold SPECT/CT) with IV injection of [^{99m}Tc] Tc-MDP. In order to determine radiopharmaceutical activity used EANM pediatric dosage card [21]. All patients underwent blood pool phase imaging around 5 minutes and delay phase imaging about 3 to 4 hours after injection of radiopharmaceutical. All image sets were analyzed twice by a nuclear medicine scientist, expert in pediatric rheumatologic disorders blinded to specific clinical information. Within our exploration of optimal count ratios for diagnosing arthritis in JIA patients, our findings was congruent with visual interpretation of adult rheumatoid arthritis images as the normal synovial surfaces are photopenic in comparison to capillary blood pool of adjacent muscles and when the count ratio within the synovial area of the knee joint exceeds the soft tissue count of the thigh, it strongly indicated an escalated probability of joint inflammation, aligning with current insights. Joint inflammation was approved by dedicated pediatric rheumatologist according to clinical symptoms, physical examinations and laboratory findings and clinical follow up evaluations.

Segmentation

Segmentation of regions of interest (ROI) is the most challenging component of a Computer-Aided Diagnosis (CAD) system and is crucial for making accurate diagnoses. It is impossible to segment the knee joint precisely in blood pool images. Therefore, for the sake of reproducibility and repeatability in image feature extraction, we chose the area between the two knee growth plates as the ROI. In this study, each knee was considered a separate sample for feature extraction. Figure 3 displays the selected ROIs. The images were manually segmented using the 3D Slicer software platform (http://slicer.org, version 5.2.1) [22] .

Image preprocessing and features extraction

Texture feature sets must be interpolated to isotropic voxel spacing to achieve rotational invariance and to allow comparisons between image information from various samples, cohorts, or batches. Maintaining constant isotropic voxel spacing across different tests and devices is crucial for repeatability. In this study,

we applied nearest neighbor interpolation to the image matrix. Briefly, nearest neighbor interpolation assigns the brightness of the closest voxel in the original grid to every voxel in the interpolation grid [23]. PyRadiomics (version 3.0.1) was used to extract several radiomic features, including texture and first-order features, in accordance with the imaging biomarker standardization initiative (IBSI) [24]. Table 1 displays the feature classes extracted from the ROI. To characterize the attributes of voxel intensities, first-order features such as energy, entropy, standard deviation, skewness, kurtosis, etc., are determined based on the intensity distribution and histogram. Texture analysis quantifies the gray-level pattern and pixel interactions. Additionally, images processed with Laplacian of Gaussian (LoG) were also analyzed.

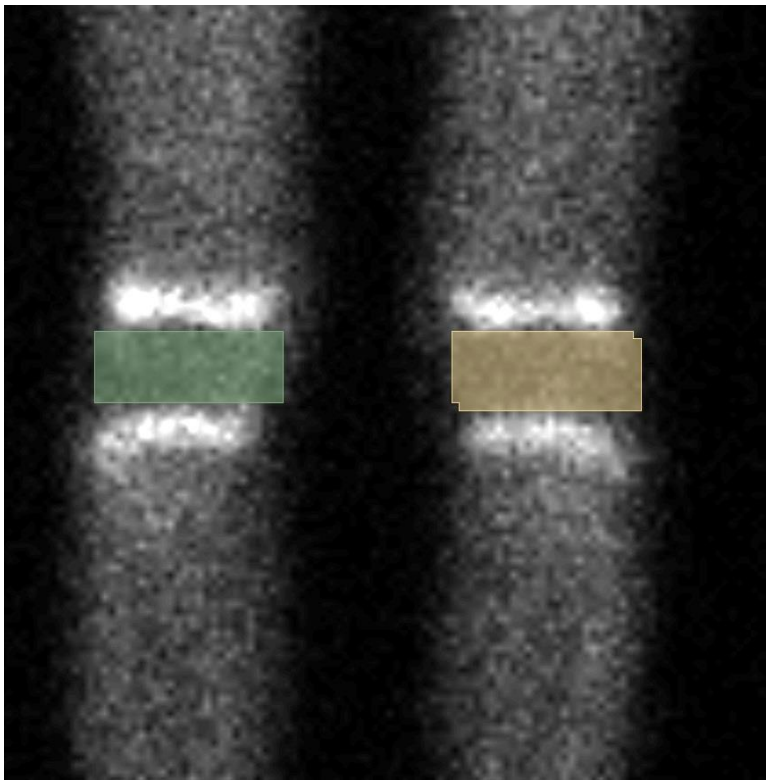

Figure 3. Image ROI for features extraction

Table 1. Feature classes extracted from blood pool images

Features Class	Numbers
First Order	18
Texture	
Gray level co-occurrence matrices (GLCM)	22
Gray level dependence matrices (GLDM)	14
Gray level size zone matrices (GLSZM)	16
Gray-level run-length matrices (GLRLM)	16
Neighboring gray-tone difference matrices (NGTDM)	5

Features selection

When working with high-dimensional data, the learning task becomes more challenging due to redundancy among features, which lowers classification accuracy and increases computational costs. In this study, the random forest recursive feature elimination (RFE) method was used to identify the most suitable features for classifying patients. RFE is a popular approach because it is straightforward to implement and effective in selecting features. It's important to note that when using RFE, choosing the number of features to select is a critical decision. The RFE technique involves training a machine learning algorithm, ranking the features based on their importance, discarding the least significant ones, and retraining the model until only a specified

number of features remain. In this study, we first removed highly correlated features (Spearman's rank correlation coefficient > 0.85) and then tested the performance of several feature sets D= (10, 11, 12, …, 20), finally selecting the optimal feature set for model building.

Model building and model evaluation

The random forest (RF) algorithm is used to classify patients as either positive or negative for Juvenile Idiopathic Arthritis (JIA). Studies have shown that the RF algorithm can effectively predict outcomes even with a small number of samples and in datasets with a vast number of dimensions [25]. In this study, 8 different models were created and evaluated with features extracted from the anterior and posterior of original and log-filtered images, as well as concatenated features from both original and filtered images, in addition to clinical features (sex and age). The models were evaluated using the area under the ROC curve and accuracy metrics. The total samples were split into 85% for training and 15% for testing, based on the learning curve. The models' hyperparameters were tuned using a 10-fold cross-validation method. To avoid data leakage, feature selection and model building were performed on the training set.

RESULTS

Patient's characteristics

In our study, we analyzed a total of 360 knee samples. Of these, 181 samples were classified as healthy, representing 50.28% of the total. The remaining 179 samples were identified as affected by the condition under investigation, accounting for 49.72% of the overall sample size. Moreover, 40% are bilaterally arthritic, and approximately 10% are unilaterally arthritic. This distribution highlights a nearly equal representation of healthy and affected knees within our study cohort, allowing for a balanced comparison and analysis. Age and sex distribution was not statistically different between the negative and positive group (P > 0.05).

Feature selection and model building

In feature selection step, we test model accuracy of different feature sets with RFE method to finally select optimal performance. For different models, number of optimal features were variable. Performances of the original, log filtered and concatenated model are presented in Table 2. As you can see the concatenated anterior original and log filtered model is the best performance model. This outperformance model constructed with 14 features including, 4 original features (*firstorder_Skewness, glcm_Autocorrelation, glcm_ClusterShade, glszm_LargeAreaEmphasis)* and 10 LoG filtered features *(firstorder_Mean, firstorder_Median, firstorder_Entropy, firstorder_10Percentile, firstorder_Energy, firstorder_Minimum, ngtdm_Coarseness, glcm_Correlation, glrlm_LongRunLowGrayLevelEmphasis, glrlm_ShortRunLowGrayLevelEmphasis*).

Table 2. Performance metrics of different model configurations

Model	AUC	ACC
Ant Original Model	0.72	0.73
Post Original Model	0.55	0.57
Concat Ant and Post Original Model	0.75	0.77
Ant LoG Filtered Model	0.80	0.81
Post LoG Filtered Model	0.61	0.63
Concat Ant and Post LoG Filtered Model	0.75	0.75
Concat Ant Original and LoG Filtered Model	0.89	0.90
Concat Post Original and LoG Filtered Model	0.60	0.62

Figure 4 illustrates the evaluation of the effectiveness of the original and combined models was done by measuring the area under the receiver operating characteristic curve (AUC) obtained from the 53 test datasets. The AUC of the concatenated anterior original and log filtered model was 0.88 (95% confidence interval (CI), 0.86 to 0.91) in the test cohort.

A learning curve is the relationship between a learning model on a task and the amount of data. Variable-sized subsets of the training set will be utilized to train the estimator, and a score will be produced for each test set. Figure 5 demonstrated the test score rises as the training dataset grows in size. In fact, it grows indicates that additional data to train the model, increase its generalization performance.

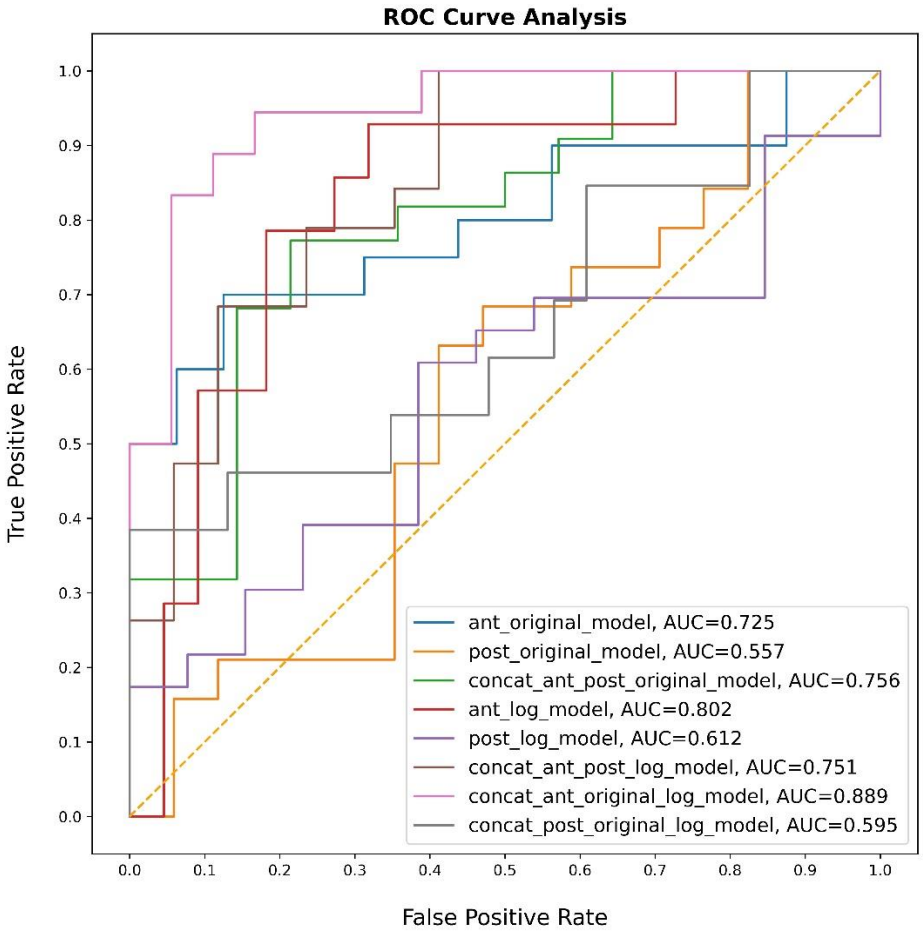

Figure 4. Area under the receiver operating characteristic curve (AUC) for primary and concatenated model

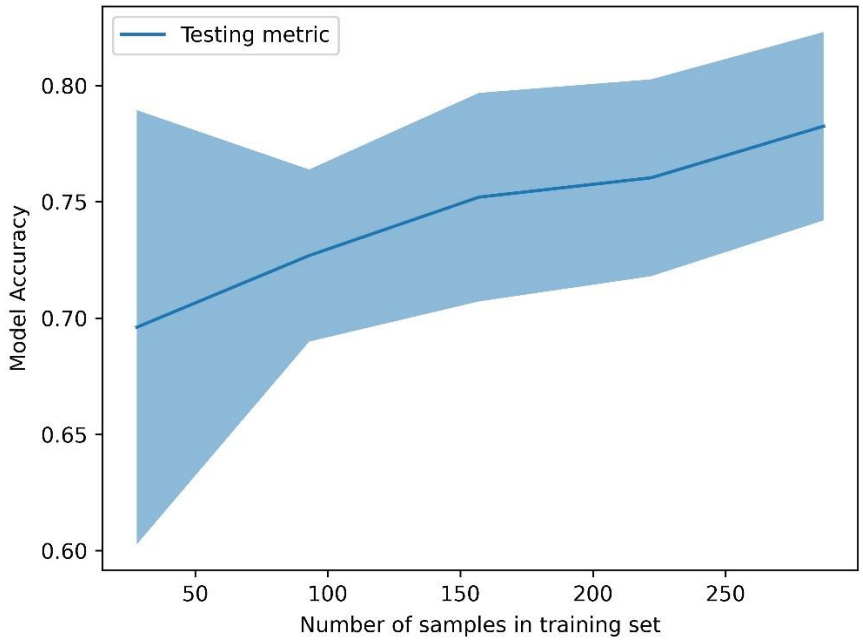

Figure 5. Learning curve RF algorithm on concatenated original and log filtered features

DISCUSSION

Medical research is constantly evolving, with -omics being conducted every day to explore different disorders. The juvenile idiopathic arthritis (JIA) is characterized by chronic mono-oligo or poly articular joint inflammation which may progress to

joint destruction and functional disability [26, 27]. This study proves that radiomics assessment on [^{99m}Tc] Tc-MDP Blood pool knee images, considered as the most involved joint in JIA [28], provides highly accurate results along with the optimal model (Concat_original_log_model) showing AUC of 0.89 and accuracy of 0.9.

In line with the importance of adhering to international rheumatology guidelines to establish standardized diagnostic criteria for Juvenile Idiopathic Arthritis (JIA), our study acknowledges the potential for further clarity in defining the standard of truth for knee arthritis diagnosis. Our diagnostic criteria were founded upon a fusion of positive blood pool imaging in scintigraphy and corroborating assessments by experienced pediatric rheumatologists. Notably, the concern raised about the possible identification of subclinical arthritis solely through scintigraphy, independent of clinical recognition by referring physicians, is a pertinent consideration. It is acknowledged that scintigraphy, as an imaging modality, may unveil subclinical alterations that elude detection during routine clinical evaluation. Our dataset encompasses instances where scintigraphy was performed due to non-articular pathologies, potentially revealing subclinical changes not clinically identified as arthritis. This underscores the need for a nuanced approach that amalgamates objective imaging findings with clinical judgment, a facet we aim to refine in future investigations.

According to our results, the combined model including anterior original and filtered image features reveal significant high performance among models (accuracy: ant_original_model = 0.72, ant_log_model = 0.81 and concat_original_log_model = 0.90). As is clear from the results, anterior image features have considerable diagnostic information rather than posterior image features that would be possibly due to angiographic scatter of popliteal arteries over posterior views. Like previous studies, [29, 30]. We demonstrate Laplacian of Gaussian (LoG) preprocessing filters positive impact on diagnostic and predictive performance of the radiomics models.

According to previous studies, [^{99m}Tc] Tc-MDP accumulates in active arthritic joints even with no clinical manifestations [31, 32]. Kim et al.'s findings indicating a 10% sensitivity increase (84% versus 74.8%) in blood pool views of 99m Tc MDP underscored the importance of this phase compared to the delay phase [14]. Our study's primary emphasis was on standardizing interpretation methodologies to ensure assessment consistency and reliability of blood pool phase. Considering the significance of inflammatory joint disease in young individuals, meticulous bone scan interpretation holds potential for early detection and monitoring the progression of JIA. Further clinical investigations in this area are essential to refine diagnostic accuracy, leading to alterations in JIA managements. The use of quantitative analysis in bone scintigraphy of rheumatoid arthritis patients has been previously studied by Lee et al., using joint uptake ratio showing 78% AUC for detecting active knee arthritis [33]; while the -omics optimal model (Concat_original_log_model) in current study shows added AUC value of about 12% in detecting active knee joints. To the best of our researches, most other studies dealt with visually interpreting bone scintigraphy images in patients with joint disorders owing inherent limitations, reported significant discrepancies among different readers [11, 34].

There are some limitations in the study that must be acknowledged. Firstly, it was a single center trial with limited number of joint views. The other limitation is monoarticular nature of this study; Future research can be performed on blood pool database of other joints involved in JIA including hip joints, ankles, wrists, etc.

CONCLUSION

This study retrospectively proved the high accuracy of radiomics in detecting active knee arthritis using [^{99m}Tc]Tc-MDP blood pool images of patients with JIA. Diagnostic robustness of radiomics in arthritic joints can shed light on future studies as an optimal alternate to available conventional quantifications.

REFERENCES

1. Petty RE, Southwood TR, Manners P, Baum J, Glass DN, Goldenberg J, He X, Maldonado-Cocco J, Orozco-Alcala J, Prieur AM, Suarez-Almazor ME, Woo P. International League of Associations for Rheumatology classification of juvenile idiopathic arthritis: second revision, Edmonton, 2001. J Rheumatol. 2004;31(2):390-2.
2. Giancane G, Consolaro A, Lanni S, Davì S, Schiappapietra B, Ravelli A. Juvenile idiopathic arthritis: diagnosis and treatment. Rheumatol Ther. 2016;3(2):187-207.
3. Prince FHM, Otten MH, Suijlekom-Smit LWAv. Diagnosis and management of juvenile idiopathic arthritis. Brit Med J. 2010;341:c6434.
4. Packham JC, Hall MA. Long-term follow-up of 246 adults with juvenile idiopathic arthritis: functional outcome. Rheumatology (Oxford). 2002;41(12):1428-35.
5. Gardner-Medwin JM, Irwin G, Johnson K. MRI in juvenile idiopathic arthritis and juvenile dermatomyositis. Ann N Y Acad Sci. 2009;1154:52-83.
6. McKay GM, Cox LA, Long BW. Imaging juvenile idiopathic arthritis: assessing the modalities. Radiol Technol. 2010;81(4):318-27.
7. Gylys-Morin VM, Graham TB, Blebea JS, Dardzinski BJ, Laor T, Johnson ND, Oestreich AE, Passo MH. Knee in early

juvenile rheumatoid arthritis: MR imaging findings. Radiology. 2001;220(3):696-706.
8. Sudoł-Szopińska I, Kontny E, Maśliński W, Prochorec-Sobieszek M, Kwiatkowska B, Zaniewicz-Kaniewska K, Warczyńska A. The pathogenesis of rheumatoid arthritis in radiological studies. Part I: Formation of inflammatory infiltrates within the synovial membrane. J Ultrason. 2012;12(49):202-13.
9. Ostrowska M, Maśliński W, Prochorec-Sobieszek M, Nieciecki M, Sudoł-Szopińska I. Cartilage and bone damage in rheumatoid arthritis. Reumatologia. 2018;56(2):111-20.
10. Ording Muller L-S, Humphries P, Rosendahl K. The joints in juvenile idiopathic arthritis. Insights Imaging. 2015;6(3):275-84.
11. Lee JW, Jung KJ, Lee SM, Chang SH. Clinical use of quantitative analysis of bone scintigraphy to assess the involvement of arthritis diseases in patients with joint symptoms. Diagnostics. 2020;10(12):1000.
12. Yoo IR. Bone SPECT/CT of the foot and ankle: potential clinical application for chronic foot pain. Eur J Nucl Med Mol I. 2020;54(1):1-8.
13. Sandrock D, Backhaus M, Burmester G, Munz DL. Imaging techniques in rheumatology: scintigraphy in rheumatoid arthritis. Z Rheumatol. 2003;62:476-80.
14. Kim JY, Choi YY, Kim CW, Sung Y-K, Yoo D-H. Bone scintigraphy in the diagnosis of rheumatoid arthritis: is there additional value of bone scintigraphy with blood pool phase over conventional bone scintigraphy?. J Korean Med Sci. 2016;31(4):502-9.
15. Gillies RJ, Kinahan PE, Hricak H. Radiomics: images are more than pictures, they are data. Radiology. 2016;278(2):563-77.
16. Lambin P, Leijenaar RTH, Deist TM, Peerlings J, de Jong EEC, van Timmeren J, Sanduleanu S, Larue RTHM, Even AJG, Jochems A, van Wijk Y, Woodruff H, van Soest J, Lustberg T, Roelofs E, van Elmpt W, Dekker A, Mottaghy FM, Wildberger JE, Walsh S. Radiomics: the bridge between medical imaging and personalized medicine. Nat Rev Clin Oncol. 2017;14(12):749-62.
17. van Timmeren JE, Cester D, Tanadini-Lang S, Alkadhi H, Baessler B. Radiomics in medical imaging-"how-to" guide and critical reflection. Insights Imaging. 2020 Aug 12;11(1):91.
18. Papathanassiou D, Bruna-Muraille C, Jouannaud C, Gagneux-Lemoussu L, Eschard JP, Liehn JC. Single-photon emission computed tomography combined with computed tomography (SPECT/CT) in bone diseases. Jt Bone Spine. 2009;76(5):474-80.
19. Masaoka S. Evaluation of arterial obstructive leg and foot disease by three-phase bone scintigraphy. Ann Nucl Med. 2001;15:281-7.
20. Cohen JF, Korevaar DA, Altman DG, Bruns DE, Gatsonis CA, Hooft L, Irwig L, Levine D, Reitsma JB, de Vet HC, Bossuyt PM. STARD 2015 guidelines for reporting diagnostic accuracy studies: explanation and elaboration. BMJ Open. 2016;6(11):e012799.
21. Lassmann M, Biassoni L, Monsieurs M, Franzius C. The new EANM paediatric dosage card: additional notes with respect to F-18. Eur J Nucl Med Mol Imaging. 2008;35(9):1666-8.
22. Fedorov A, Beichel R, Kalpathy-Cramer J, Finet J, Fillion-Robin J-C, Pujol S, Bauer C, Jennings D, Fennessy F, Sonka M, Buatti J, Aylward S, Miller JV, Pieper S, Kikinis R. 3D Slicer as an image computing platform for the Quantitative Imaging Network. Magn Reson Imaging. 2012;30(9):1323-41.
23. Thévenaz P, Blue T, Unser M. Image interpolation and resampling. In: Handbook of Medical Imaging, Processing and Analysis. New York: Academic. 2000. p. 393–420.
24. Zwanenburg A, Vallières M, Abdalah MA, Aerts HJWL, Andrearczyk V, Apte A, Ashrafinia S, Bakas S, Beukinga RJ, Boellaard R, Bogowicz M, Boldrini L, Buvat I, Cook GJR, Davatzikos C, Depeursinge A, Desseroit M-C, Dinapoli N, Dinh CV, Echegaray S, Naqa IE, Fedorov AY, Gatta R, Gillies RJ, Goh V, Götz M, Guckenberger M, Ha SM, Hatt M, Isensee F, Lambin P, Leger S, Leijenaar RTH, Lenkowicz J, Lippert F, Losnegård A, Maier-Hein KH, Morin O, Müller H, Napel S, Nioche C, Orlhac F, Pati S, Pfaehler EAG, Rahmim A, Rao AUK, Scherer J, Siddique MM, Sijtsema NM, Fernandez JS, Spezi E, Steenbakkers RJHM, Tanadini-Lang S, Thorwarth D, Troost EGC, Upadhaya T, Valentini V, Dijk LVv, Griethuysen Jv, Velden FHPv, Whybra P, Richter C, Löck S. The image biomarker standardization initiative: standardized quantitative radiomics for high-throughput image-based phenotyping. Radiology. 2020;295(2):328-38.
25. Biau G, Scornet E. A random forest guided tour. Test. 2016;25(2):197-227.
26. Alam J, Jantan I, Bukhari SNA. Rheumatoid arthritis: recent advances on its etiology, role of cytokines and pharmacotherapy. Biomedicine & Pharmacotherapy. 2017;92:615-33.
27. Goronzy JJ, Weyand CM. Developments in the scientific understanding of rheumatoid arthritis. Arthritis Res Ther. 2009;11(5):1-14.
28. Hemke R, Nusman CM, van der Heijde DM, Doria AS, Kuijpers TW, Maas M, van Rossum MA. Frequency of joint involvement in juvenile idiopathic arthritis during a 5-year follow-up of newly diagnosed patients: implications for MR imaging as outcome measure. Rheumatol Int. 2015;35(2):351-7.
29. Demircioğlu A. The effect of preprocessing filters on predictive performance in radiomics. Eur Radiol Exp. 2022 Dec;6(1):40.
30. Patra J, Moulick HN, Manna AK. Medical Image Processing in Nuclear Medicine and Bone Arthroplasty. IOSR J Comput Eng. 2013;13(2):97-110.
31. Berná L, Torres G, Diez C, Estorch M, Martínez-Duncker D, Carrió I. Technetium-99m human polyclonal immunoglobulin G studies and conventional bone scans to detect active joint inflammation in chronic rheumatoid arthritis. Eur J Nucl Med. 1992;19:173-6.
32. Fisher B, Frank J, Taylor P. Do Tc-99m-diphosphonate bone scans have any place in the investigation of polyarthralgia?. Rheumatology. 2007; 46 (6): 1036–7.
33. Lee JW, Chang SH, Jang SJ, Park HJ, Lee SM, Jung KJ. Clinical utility of quantitative analysis of bone scintigraphy in detecting clinically active joint and high disease activity in patients with rheumatoid arthritis. BMC Med Imaging. 2021;21(1):177.
34. Kim JY, Cho S-K, Han M, Choi YY, Bae S-C, Sung Y-K. The role of bone scintigraphy in the diagnosis of rheumatoid arthritis according to the 2010 ACR/EULAR classification criteria. J Korean Med Sci. 2014;29(2):204-9.